JOURNAL OF EXPERIMENTAL AND THEORETICAL PHYSICS, 2025, Vol. 167, No. 1, pp. 136–142

STATISTICAL, NONLINEAR, AND SOFT MATTER PHYSICS

RESONANT WAVEGUIDE LUMINESCENCE LOSSES IN A LIQUID CRYSTAL LAYER CONFINED BY ITO ELECTRODES

© 2025 S. P. Palto, D. O. Rybakov, A. R. Geivandov*, I. V. Kasyanova

Shubnikov Institute of Crystallography, Kurchatovsky Complex "Crystallography and Photonics" National Research Centre Kurchatov Institute, Moscow, Russia

**e-mail: ageivandov@yandex.ru*

Received August 15, 2024

Revised September 05, 2024

Accepted September 05, 2024

Abstract. In a planarly-aligned layer of a nematic liquid crystal (LC) with a luminescent dye, the spectra of luminescence arising upon laser excitation of dye molecules and propagating in the waveguide mode were investigated. It was shown that the presence of ITO electrodes confining the LC layer leads to significant resonant losses of radiation energy. These losses are explained by phase synchronism between the waveguide modes in the LC layer and the ITO electrodes. The spectral position of the loss maxima depends on the polarization state of light, and their intensity increases with decreasing LC layer thickness. It was shown that the use of LC alignment layers made of fluorinated polymers with a low refractive index coated onto ITO electrodes allows one to significantly suppress resonant radiation losses.

Keywords: *liquid crystal, ITO losses, waveguide mode, luminescence, LC lasing*

DOI: 10.31857/S00444510250112e6

1. INTRODUCTION

Alongside the widespread use of liquid crystals (LCs) in information display technologies, there has been increasing interest in utilizing LCs for various photonic devices. In particular, LC materials doped with laser dyes can be employed both for studying the photonic properties of LCs [1, 2] and as an active medium for microlaser systems [3, 4, 5, 6, 7]. Among these systems, microlasers operating in the waveguide light generation mode hold a special place [8, 9, 10, 11, 12]. However, despite the many advantages of the waveguide generation mode, this approach also has certain drawbacks. For example, controlling the LC layer to create spatially periodic refractive index modulation and, consequently, distributed feedback, requires control electrodes that confine the LC layer. In LC devices, transparent electrodes based on indium tin oxide (ITO) are widely used. In this case, an inevitable problem arises due to the need to minimize light energy losses in the electrodes during waveguide mode propagation.

In [13], numerical FDTD modeling demonstrated that light propagation in the waveguide mode within oriented LC layers confined by transparent ITO electrodes is characterized by significant resonant losses. These losses occur in specific spectral ranges due to phase-synchronous energy transfer from the liquid crystal layer to the thin electrode layers. The present study aims to experimentally observe the resonant losses predicted in [13] by exciting luminescence in the LC layer and recording the luminescence spectrum at the output of the liquid crystal waveguide formed by the LC layer and the confining layers, including ITO. The study also investigates the possibility of reducing these losses by introducing alignment layers with a low refractive index between the ITO electrodes and the LC layer, as recommended in [13].

2. EXPERIMENTAL SAMPLES

The experimental scheme of the liquid crystal (LC) cell with ITO electrodes is shown in Fig. 1. The cell consists of two glass substrates 1, 2, with transparent ITO electrodes 3, 4 at their inner sides.

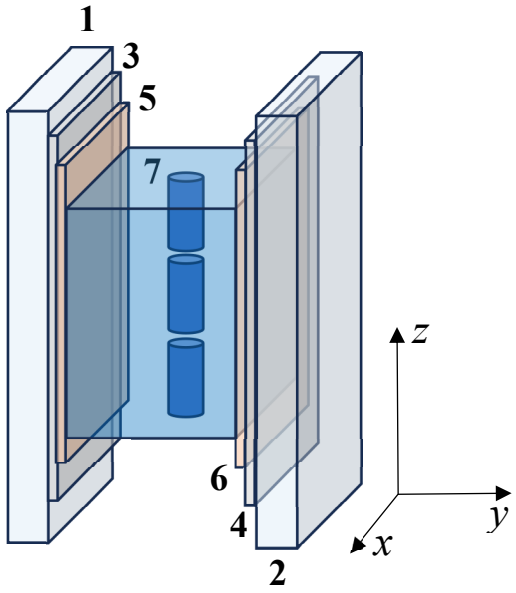

Fig. 1. Schematic diagram of the layered structure of the LC cell. *1*, *2* – glass substrates; *3*, *4* – ITO electrode layers; *5*, *6* – polymer alignment layers rubbed in the direction *z*; *7* – LC layer (E7) with DCM dye (cylinder axes indicate the LC director direction).

We used industrial glass for display technologies with a measured ITO electrode thickness of 150 ± 10 nm. To achieve planar alignment of the nematic LC (E7, Merck), thin polymer films 5, 6 were applied to the ITO surfaces and mechanically rubbed with a soft cloth along the *z*-axis, determining the easy axis direction and, consequently, the optical axis direction in the LC layer. Two types of polymers were used for the alignment films: (a) polyimide (PI) with a refractive index of 1.65 (AD9103 lacquer, NPO Plastik) and (b) fluorinated polymer with a refractive index of 1.42 (copolymer of tetrafluoroethylene and vinylidene fluoride, F42-V). The LC layer thickness, alignment film type, and presence of ITO electrodes varied depending on the sample number (see table).

As seen from the table, Sample 1 does not contain ITO electrodes. This LC cell was used as a reference sample to visualize spectral changes in the emitted light due to the presence of ITO electrodes.

The choice of the liquid crystal E7 is due to the extensive study of this material and the availability of many of its physical parameters. For example, the spectral dependencies of the refractive index, crucial for our studies, are well known across a wide

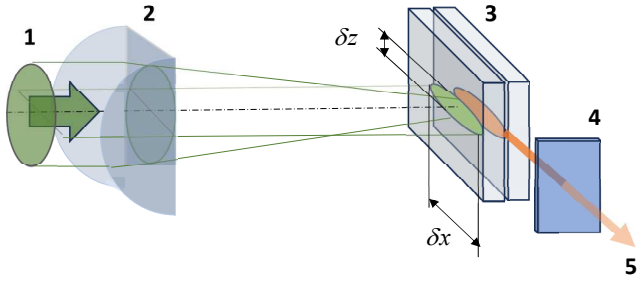

Fig. 2. Scheme of luminescence excitation in the LC layer. *1* – laser beam (λ = 532 nm, τ = 10 ns); *2* – cylindrical lens (focal length *f* = 100 mm, characteristic focusing area dimensions δ*z* = 0.1 mm; δ*x* = 3 mm); *3* – liquid crystal cell; *4* – set of optical filters and polarizer; *5* – radiation registered by a fiber optic spectrometer.

spectral range [14], allowing us to build a realistic model of resonant losses in the E7 layer between ITO electrodes in [13]. To impart luminescent properties to the LC layer, we used the well-known laser dye DCM (4-(Dicyanomethylene)-2-methyl-6-(4-dimethylaminostyryl)-4H-pyran, Sigma Aldrich, 0.6 wt.%). This dye is characterized by intense luminescence in the 570–650 nm wavelength range and is widely used to achieve lasing effects in various LC systems.

The luminescence excitation and registration scheme is shown in Fig. 2. Luminescence excitation in the LC layer was performed using radiation 1 from a neodymium laser operating in Q-switched mode at a wavelength of λ=532 nm with a pulse duration of 10 ns. The pulse energy was approximately 80 μJ. The laser radiation was linearly polarized along the direction z (along the LC director), ensuring maximum luminescence efficiency [11]. The laser beam was focused on the LC layer in cell 3 by cylindrical lens 2 into a narrow stripe with a width of $\delta z = 0.1$ mm and a length of $\delta x = 3$ mm along the direction x of waveguide luminescence propagation 5. The position x_0 of the focused area center, measured from the LC cell end, varied from 1.5 to 2.5 mm.

Luminescence from the LC layer end face was recorded using a fiber optic spectrometer Avantes Avaspec 2048. To exclude the registration of light propagating into the substrates, the ends of the latter were coated with an opaque (black) dye layer, and a mask with a slit was used. To register polarization spectra, a polarizer 4 was placed in

Table. Analyzed samples and their parameters

Sample No.	LC layer thickness, μm	Sample type	Alignment layer thickness, nm	ITO presence
1	6.7 ± 0.2	PI	20 ± 10	No
2	6.8 ± 0.2	PI	20 ± 10	Yes
3	2.4 ± 0.2	PI	20 ± 10	Yes
4	12 ± 0.2	PI	20 ± 10	Yes
5	6.3 ± 0.2	Ф42-В	350 ± 10	Yes

front of the fiber optic cable lens, allowing the recording of TE-polarized spectra (electric field oscillations along the z axis and LC director, see Fig. 1) and TM-polarized spectra (electric field oscillations in the xy plane). Additionally, glass optical filters were used to attenuate both scattered laser radiation and luminescence when necessary, installed alongside the polarizer in front of the fiber optic cable input lens of the spectrometer.

3. DISCUSSION OF RESULTS

Fig. 3 shows the spectra of unpolarized luminescence for the reference sample 1 (see table) without ITO electrodes (curve 1) and sample 2 (curve 2), obtained under identical laser excitation pulse energies (approximately 80 μJ). It is worth noting that the luminescence intensity here and below is presented on a logarithmic scale. As seen, the luminescence intensity for sample 2 with ITO electrodes is significantly lower than that recorded for the reference sample 1. In the spectrum (curve 2), a characteristic dip at the wavelength of 588 nm is observed, which is absent in the sample without ITO. When the spectrum of sample 2 is divided by the spectrum of sample 1, the spectral dependence of the relative losses I_2/I_1 in sample 2 compared to sample 1 is obtained (see the inset in Fig. 3).

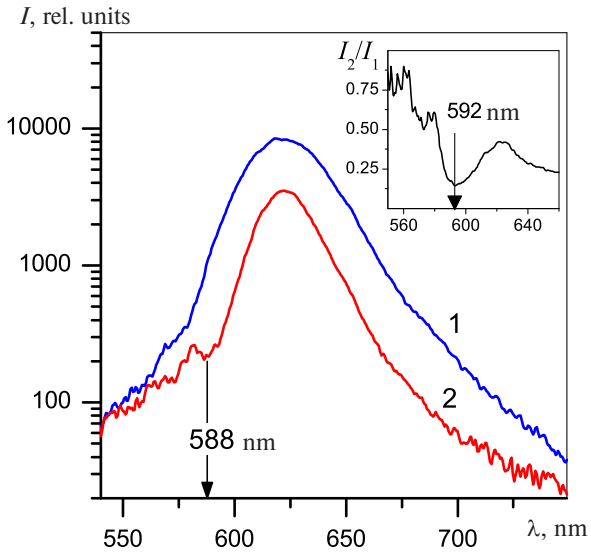

Fig. 3. Luminescence spectra at the output of the LC cell (see Fig. 2) after light propagation in the LC layer in the waveguide mode. The pump area length determining the propagation distance is $\delta x = 3$ mm, and the distance from the pump center to the LC cell edge is $x_0 = 1.5$ mm. Curve *1* – spectrum of sample 1 (no ITO electrodes); curve *2* – spectrum of sample 2 (with ITO electrodes, thickness 150 nm). The inset shows the ratio of the spectrum of sample 2 to that of sample 1.

It is evident that the relative losses associated with the presence of ITO electrodes are characterized by a spectral band with a maximum absorption at the wavelength of 592 nm. The luminescence intensity at this wavelength for sample 2 is approximately 8 times lower than that for sample 1. There is also an increase in losses at wavelengths longer than 625 nm. Unfortunately, it is challenging to register this longer-wavelength band accurately across the entire range due to the very low luminescence intensity at wavelengths above 650 nm.

According to the numerical calculations in [13] for a planarly-aligned liquid crystal layer E7 confined by ITO electrodes with a thickness of 170 nm, two resonance bands exist in the spectral range of 550–900 nm, with maximum losses at wavelengths of волн $\lambda_1 = 570$ nm and $\lambda_2 = 705$ nm for TE- and TM-polarized light, respectively. The spectral position of these losses does not depend on the thickness of the LC layer. However, as shown in [13], changes in the ITO layer thickness and

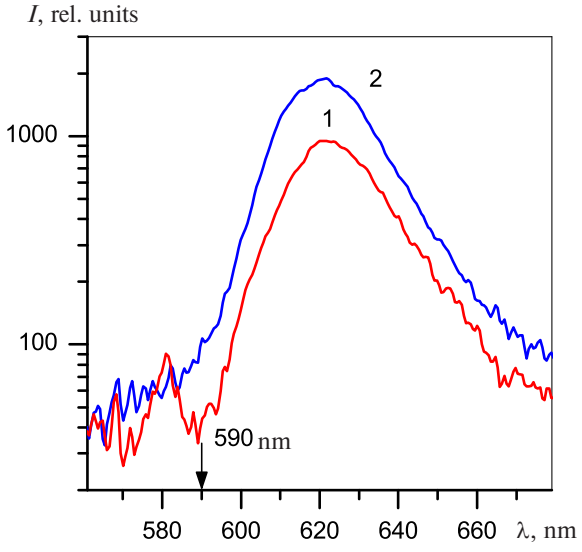

Fig. 4. Polarization spectra of luminescence measured for sample 1, where curve *1* corresponds to TE-polarization and curve *2* to TM-polarization. The distance from the pump center to the LC cell edge is $x_0 = 1.5$ mm.

the presence of a polyimide alignment film can shift the spectral position of the resonance bands. Considering the experimental error associated with measuring the ITO layer thickness and the presence of a thin polyimide alignment film in experimental sample 2, we associate the observed loss maximum at 592 nm with the resonance band calculated at $\lambda_1 = 570$ nm for the TE-polarized mode in [13]. Similarly, the increasing losses at wavelengths above 625 nm (inset in Fig. 3) are explained by the calculated resonance band at $\lambda_2 = 705$ nm for TM-polarized light. The spectral data in Fig. 4, showing the polarization spectra of luminescence, confirm this conclusion. The luminescence intensity dip at 588 nm is characteristic only for the TE-polarized mode (curve 1 in Fig. 4). As the wavelength increases beyond 625 nm, the intensity of TM-polarized luminescence, shown by curve 2, decreases faster than that of the TE mode (curve 1). Thus, the observed long-wavelength losses also agree with the numerical model in [13].

According to the analytical model of a thin ITO layer with a refractive index n_1 between the glass substrate n_0 and the liquid crystal layer n_2, the wavelengths corresponding to the maxima of the resonance losses are determined by the following relations [13]:

$$\lambda_{m,TE,TM} = \frac{2d_{ITO}n_2}{m - \frac{\delta\phi_{TE,TM}}{2\pi}} \times \sqrt{\left(\frac{n_1}{n_{2,TE,TM}}\right)^2 - 1}, \quad (1)$$

where the indices TE and TM refer to TE- and TM-polarized light, respectively, and m is a natural number. The additional phase shifts $\delta\phi$ in Equation (1), associated with double reflection of waves in the ITO layer from the boundaries of the ITO-glass substrate and the ITO-LC layer interfaces, are determined for TE- and TM-polarized light by the following expressions:

$$\delta\phi_{TE} = -2\left[arctg\left(\frac{\sqrt{\sin^2(\theta_{1,TE}) - (\frac{n_0}{n_1})^2}}{\cos(\theta_{1,TE})}\right) + arctg\left(\frac{\sqrt{\sin^2(\theta_{1,TE}) - (\frac{n_{2,TE}}{n_1})^2}}{\cos(\theta_{1,TE})}\right)\right],$$

$$\delta\phi_{TM} = 2\pi - 2\left[arctg\left(\frac{\sqrt{\sin^2(\theta_{1,TM}) - (\frac{n_0}{n_1})^2}}{(\frac{n_0}{n_1})^2\cos(\theta_{1,TM})}\right) + arctg\left(\frac{\sqrt{\sin^2(\theta_{1,TM}) - (\frac{n_{2,TM}}{n_1})^2}}{(\frac{n_{2,TM}}{n_1})^2\cos(\theta_{1,TM})}\right)\right].$$

It is also important to consider the spectral dispersion of refractive indices: $n_0 \equiv n_0(\lambda)$ is the refractive index of the glass substrate, $n_1 \equiv n_1(\lambda)$ is the refractive index of ITO, $n_{2,TE,TM} \equiv n_{2,TE,TM}(\lambda)$ is the polarization-dependent refractive index of the liquid crystal (for planarly-aligned LC, $n_{2,TE} = n_{\parallel}$, $n_{2,TM} = n_{\perp}$), θ_1 is the angle between the layer normal and the wave vector in the ITO layer (for phase-synchronized coupling of the planar mode from the LC layer to the ITO, $\sin\theta_1 = n_1 / n_{2,TE,TM}$).

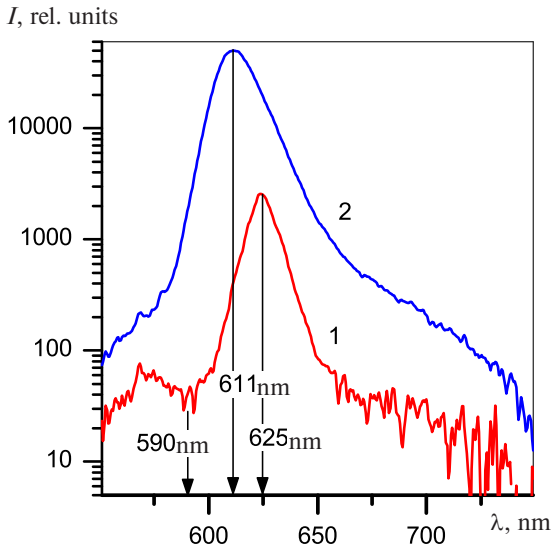

Fig. 5. Spectra of unpolarized luminescence for sample 3 (curve *1* $d = 2.4$ μm) and sample 4 (curve *2*, $d = 12$ μm). Distance from the pump center to the LC cell edge is $x_0 = 2.5$ mm.

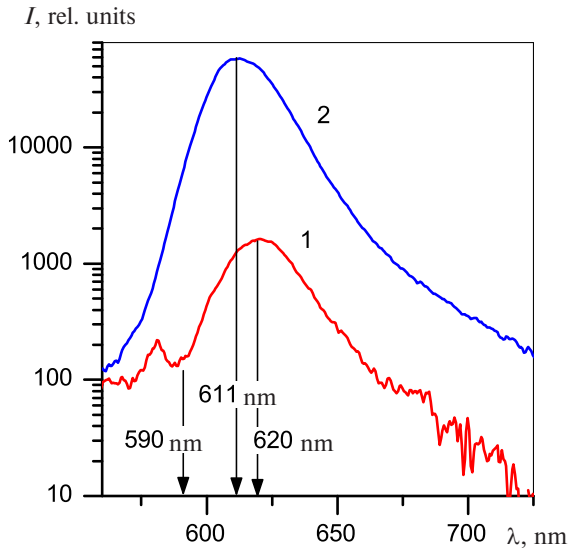

Fig. 6. Spectra of unpolarized luminescence for sample 2 (curve *1*, $d = 6.8$ μm) and sample 5 (curve *2*, $d = 6.3$ μm). Distance from the pump center to the LC cell edge $x_0 = 2.5$ mm.

As follows from Equation (1), real solutions exist only under the condition $n_1 \geq n_2$. For ITO, there is strong spectral dispersion of the refractive index [13], so the corresponding solutions exist only in specific spectral ranges, which differ for TE- and TM-polarized light due to the optical anisotropy of the liquid crystal and, accordingly, the conditions:

$$n_1 \geq n_{2,TE}, \quad n_1 \geq n_{2,TM}.$$

As shown in [13], for planar LC alignment, there are only two solutions for TM-polarized light: $\lambda_m \cong 720$ nm for $m = 1$ and $\lambda_m \cong 440$ nm for $m = 2$. Since the luminescence spectrum is limited to approximately 550–700 nm, we can observe only the short-wavelength edge of the TM mode absorption for $m = 1$, which appears at wavelengths above 625 nm (see the inset in Fig. 3).

For TE polarization, the corresponding loss peak occurs at $\lambda = 570$ nm, which, considering measurement errors and differences between our experiment and the model, is very close to the observed peak at 592 nm (see the inset in Fig. 3). In the experiment, as in the model, this loss peak is observed exclusively for TE-polarized light (Fig. 4).

The model in [13] predicts a significant increase in losses with decreasing LC layer thickness. This was confirmed experimentally (Fig. 5). Here, curve 1 corresponds to sample 3 (see table) with an LC layer thickness of $d = 2.4$ μm, and curve 2 corresponds to a thickness of $d = 12$ μm. Both curves are for unpolarized light, showing the loss peak at 592 nm and the onset of a sharp luminescence decrease at wavelengths above 625 nm, associated with the existence of a longer-wavelength loss band peaking beyond 700 nm. A comparison of luminescence intensities at 590 nm reveals that reducing the thickness from 12 to 2.4 μm increased the losses by approximately 40 times. The presence of strong loss bands for sample 3 around $\lambda_m \cong 590$ nm and in the longer-wavelength region ($\lambda_m > 700$ nm) leads to significant narrowing of the luminescence spectrum (curve 1, Fig. 5), with the luminescence maximum shifting to the longer-wavelength region near $\lambda = 625$ nm, where losses are minimal. In sample 4 (curve 2), the loss bands appear only as shoulders in the luminescence spectrum, and there is virtually no shift in the luminescence peak ($\lambda = 611$ nm). Notably, at a fixed pump energy of approximately 80 μJ, the luminescence intensity peak in sample 4 was so high that we had to shift the pump center from the LC cell edge to $x_0 = 2.5$ mm to remain within the dynamic range of the spectrometer.

Thus, the spectral measurements fully confirmed the presence of resonance losses caused by the ITO electrodes. According to the aforementioned numerical modeling, resonance losses can be significantly suppressed by introducing thin

low-refractive-index films between the LC layer and the ITO electrodes. This condition is satisfied in sample 5, where relatively thick (350 nm) fluorinated polymer F42-V films with a refractive index of 1.42 were used as LC alignment layers. The results of luminescence spectra measurements were quite impressive (Fig. 6). At a fixed pump pulse energy of 80 μJ, the peak luminescence intensity increased by approximately 50 times compared to sample 2. The characteristic loss band with a maximum at 590 nm disappeared, as did the long-wavelength spectral losses characteristic of sample 2. At wavelengths above 650 nm, luminescence increased significantly, so that even at 750 nm, the measured luminescence signal was significantly above the noise level.

To note, the luminescence intensity in sample 5 significantly exceeds not only that of sample 2 but also that of sample 1, where ITO electrodes are absent. Thus, the high luminescence intensity in sample 5 is not only due to the elimination of resonance losses. We hypothesize that another significant factor contributing to the increased luminescence intensity in sample 5 is the low refractive index of the fluoropolymer ($n = 1.42$), which is significantly lower than that of the glass substrates ($n_0 = 1.51$). As a result, a significantly larger number of TE- and TM-polarized waveguide modes can propagate in the LC layer of sample 5 compared to samples 1 and 2. Indeed, in samples 1 and 2, the lowest refractive index of the LC, $n_\perp = 1.52$, interacting with TM-polarized modes, is very close to the refractive index of the display glass (1.51). Therefore, the critical angle relative to the substrate plane, below which waveguide modes exist, is very small, causing a significant amount of TM-polarized luminescence propagating at angles above the critical angle to leak into the glass substrates.

The situation is further complicated by the fact that, in reality, the LC director does not strictly coincide with the TE polarization direction due to a slight (2–4°) pretilt angle of the director relative to the substrate plane. Thus, even TE-polarized radiation, for which the waveguide condition is satisfied over a wide range of propagation angles, partially converts into TM-polarized modes that leak into the substrate. Resonance losses, in turn, are characterized by relatively broad spectra, significantly reducing luminescence intensity even at wavelengths far from the resonance maxima. This is evident not only from the inset in Fig. 3 but also, for example, in Fig. 5 for sample 3 (curve 1), where, as already noted, significant losses on the "tails" of the resonance bands lead to spectral narrowing and a shift of the luminescence maximum. Thus, resonance losses lead to reduced luminescence across the entire spectral range. It is also worth noting that the modeling in [13], where the resonance bands are relatively narrow, was performed for a single-mode regime, where the light "injected" into the waveguide was characterized by a wave vector strictly parallel to the LC layer plane.

4. CONCLUSION

The experiment confirmed the presence of resonance losses during light propagation in waveguide mode within an LC layer confined by ITO electrodes. The observed spectral loss bands are polarization-sensitive. The spectral position of these bands does not depend on the LC layer thickness, while their intensity increases with decreasing layer thickness.

It was also demonstrated that the use of fluorinated polymer alignment layers with a low refractive index effectively suppresses resonance losses. The obtained results are significant for the application of waveguide modes in electrically controlled LC devices utilizing light propagation in waveguide mode, particularly for liquid crystal microlasers.

FUNDING

This work was carried out as part of the state assignment of the National Research Center "Kurchatov Institute."

REFERENCES

1. *P. V. Dolganov, V. K. Dolganov*. JETP Lett. **108**, 170 (2018).
2. *P. V. Dolganov*. JETP Lett. **105**, 657 (2017).
3. *I. P. Il'chishin, E. A. Tikhonov, V. G. Tishchenko et al.* JETP Lett. **32**, 24 (1980).
4. *W. Cao, A. Munos, P. Palffy-Muhoray et al*. Nature Mater. **1**, 111 (2002).
5. *A. Chanishvili, G. Chilaya, G. Petriashvili et al*. Appl. Phys. Lett. **86**, 051107 (2005).

6. *J. Ortega, C. L. Folcia, J. Etxebarria*. Materials **11**, 5 (2018).

7. *S. P. Palto, N. M. Shtykov, B. A. Umanskii et al*. J. Appl. Phys. **112**, 013105 (2012).

8. *T. Matsui, M. Ozaki, K. Yoshino*. in Proc. SPIE5518, Liquid Crystals VIII (15 October 2004).

9. *Y. Inoue, H. Yoshida, K. Inoue et al*. Appl. Phys. Express **3**, 102702 (2010).

10. *H. Yunxi, Z. Xiaojuan, Y. Benli et al*. Nanophotonics **10**, 3541 (2021).

11. *N. M. Shtykov, S. P. Palto, B. A. Umanskii et al*. Crystallography Rep. **64**, 305 (2019).

12. *N. M. Shtykov, S. P. Palto, A. R. Geivandov et al*. Opt. Lett. **45**, 4328 (2020).

13. *S. P. Palto, A. R. Geivandov*. Photonics **10**, 1089 (2023).

14. *J. Li, C.-H. Wen, S. Gauza et al*. J. of Display Technol. **1**, 52 (2005).